Biol Fertil Soils (2017) 53:287–301
DOI 10.1007/s00374-016-1174-9

ORIGINAL PAPER

Microbial decomposition of soil organic matter is mediated by quality and quantity of crop residues: mechanisms and thresholds

Muhammad Shahbaz[1,2] · **Yakov Kuzyakov**[1,3] · **Muhammad Sanaullah**[4] · **Felix Heitkamp**[2] · **Vladimir Zelenev**[5] · **Amit Kumar**[1] · **Evgenia Blagodatskaya**[1,3,6]

Received: 29 September 2016 / Revised: 20 December 2016 / Accepted: 29 December 2016 / Published online: 12 January 2017

Abstract Crop residue quality and quantity have contrasting effects on soil organic matter (SOM) decomposition, but the mechanisms explaining such priming effect (PE) are still elusive. To reveal the role of residue quality and quantity in SOM priming, we applied two rates (5.4–10.8 g kg^{-1}) of ^{13}C-labeled wheat residues (separately: leaves, stems, roots) to soil and incubated for 120 days. To distinguish PE mechanisms, labeled C was traced in CO_2 efflux and in microbial biomass and enzyme activities (involved in C, N, and P cycles) were measured during the incubation period. Regardless of residue type, PE intensity declined with increasing C additions. Roots were least mineralized but caused up to 60% higher PE compared to leaves or stems. During intensive residue mineralization (first 2–3 weeks), the low or negative PE resulted from pool substitution. Thereafter (15–60 days), a large decline in microbial biomass along with increased enzyme activity suggested that microbial necromass served as SOM primer. Finally, incorporation of SOM-derived C into remaining microbial biomass corresponded to increased enzyme activity, which is indicative of SOM cometabolism. Both PE and enzyme activities were primarily correlated with residue-metabolizing soil microorganisms. A unifying model demonstrated that PE was a function of residue mineralization, with thresholds for strong PE increase of up to 20% root, 44% stem, and 51% leaf mineralization. Thus, root mineralization has the lowest threshold for a strong PE increase. Our study emphasizes the role of residue-feeding microorganisms as active players in the PE, which are mediated by quality and quantity of crop residue additions.

Keywords ^{13}C-labeled crop residues · Enzyme activities · Litter quality · Microbial necromass · Priming effect · Soil organic matter

Electronic supplementary material The online version of this article (doi:10.1007/s00374-016-1174-9) contains supplementary material, which is available to authorized users.

✉ Muhammad Shahbaz
shahbazmu@yahoo.com

[1] Department of Agricultural Soil Sciences, Georg August University Göttingen, Büsgenweg 2, 37077 Göttingen, Germany

[2] Section of Physical Geography, Faculty of Geoscience and Geography, Georg August University Göttingen, Goldschmidtstr 5, 37077 Göttingen, Germany

[3] Department of Soil Science of Temperate Ecosystems, Georg August University Göttingen, Büsgenweg 2, 37077 Göttingen, Germany

[4] Institute of Soil and Environmental Sciences, University of Agriculture, Faisalabad, Pakistan

[5] Department of Microbiology, Biological Faculty, Moscow State University, Vorob'evy Gory, 119899 Moscow, Russia

[6] Institute of Physicochemical and Biological Problems in Soil Science, Russian Academy of Sciences, Institutskaya st., 2, 142290 Pushchino, Moscow Region, Russian Federation

Introduction

Soil organic matter (SOM) is primarily formed through the partial degradation and transformation of crop residues by microorganisms (Castellano et al. 2015). The quality and quantity of crop residues influence the microbial decomposition processes, which may affect residue and SOM mineralization rates, leading to a priming effect (PE). The PE represents the changes of native SOM decomposition as a result of exogenous substrate inputs such as crop residues (Jenkinson et al. 1985; Kuzyakov 2010). As soil microorganisms are mostly C-limited, input and/or high availability of substrates may alter their activities, resulting in a PE (Blagodatskaya and

Kuzyakov 2008). While increasing amounts of substrate addition can decrease PE, the effect, however, depends on the substrate quality (Guenet et al. 2010). If substrate composition and availability are heterogeneous (e.g., crop residues), then a cascade of apparent (due to microbial turnover) and real (due to SOM decomposition) PE can be induced over time at various stages of substrate decomposition (Kuzyakov 2010; Xu et al. 2011).

Crop residues vary in their structural and chemical composition (Aber and Melillo 1982; Adair et al. 2008). Residue decomposition rates are generally negatively related to the amount of recalcitrant compounds present in their biomass, such as lignin, phenols, and tannins (Aber and Melillo 1982; Bertrand et al. 2006; Castellano et al. 2015). Aboveground crop residues (e.g., leaves and stems) are considered of high quality compared with belowground residues, which are relatively recalcitrant to decomposition, e.g., roots (Bertrand et al. 2006; Rasse et al. 2005). The role of residue quality in SOM formation is currently under debate. The common view on recalcitrant root residues, which are decomposed slowly and therefore contribute largely to SOM (Berg and McClaugherty 2014; Johnson et al. 2014; Rasse et al. 2005), contradicts the view of the great contribution of easily decomposable residues in SOM formation (Cotrufo et al. 2013, 2015; Lehmann and Kleber 2015). The latter concept is mainly associated with the microbial by-products, which are released and stabilized in the soil mineral fraction during crop residue decomposition (Cotrufo et al. 2013; Ladd et al. 1996; Shahbaz et al. 2016b) and microbial turnover (Ladd et al. 1996; Miltner et al. 2012).

The soil microbial turnover depends on substrate quality and availability (Leifeld and von Lützow 2014; Nguyen and Marschner 2016). If substrate availability or input is interrupted, microorganisms may respond by a switch to dormancy or their biomass decreases after microbial cell death. Such a relatively fast decrease of substrate-dependent microbial biomass (MB) was already detected in several laboratory incubation experiments (e.g., Blagodatskaya et al. 2011a; Jiang-shan et al. 2005; Tian et al. 2015; Wang et al. 2016). The decrease in MB results in accumulation of microbial necromass (after their cell death), which is already considered as an important source for stable SOM (Miltner et al., 2009, 2012; Wagner 1968). Due to its heterogeneous nature, microbial necromass may serve as labile substrates for living microorganisms and its reutilization can represent SOM priming.

The PE has often been explained by the microbial activation hypothesis (Chen et al. 2014). Instead of total microorganisms, the active microbial fraction is considered to be more important (Blagodatskaya and Kuzyakov 2013). The active fraction mostly consists of the growing portion of microorganisms, which respond rapidly to substrate addition, e.g., by producing enzymes (Blagodatskaya and Kuzyakov 2013; Fontaine et al. 2007). Depending on substrate quality (i.e., labile substance or C/N ratio), the active microbial fraction produces enzymes either to degrade added organics or to decompose SOM to meet their nutritional demands (Schnecker et al. 2014; Wang et al. 2015). This, again, may result in variable successions of PE over time. The changes in microbial activity due to substrate decomposition (rapidly or slowly) can therefore be recognized, for example, by the changes in enzyme activities (Burns et al. 2013; Nannipieri et al. 2002, 2012; Schnecker et al. 2014).

Most of the studies investigating PE used labeled low molecular weight substances such as glucose and amino acids (e.g., Blagodatskaya et al. 2011a; Hoyle et al. 2008; Tian et al. 2015). Only a few studies have distinguished PE using labeled crop residues, mostly with contrasting results depending on the residue type. PE proves to be a linear function of MB but is also a saturation function of the substrate's C amount (Guenet et al. 2010; Xiao et al. 2015). Although the effect of residue quality on PE is not obvious, the role of residue-decomposing microbial fractions in PE is highlighted based on the contrasting quality of substrate additions (Wang et al. 2015). We lack information explaining the mechanisms of PE under contrasting quality and quantity of crop residue C based on the active residue-feeding microbial fraction.

The present study is designed to explain the mechanisms of PE induced by crop residues varying in their amount and quality. Here, we used homogeneously ^{13}C-labeled wheat (*Triticum aestivum* L.) biomass to partition residue- and SOM-derived C within total CO_2 and MB. We added contrasting quality wheat residues from both aboveground (leaves, stems) and belowground (roots) parts to soil at two levels. We hypothesized that (i) the intensity of SOM decomposition will be affected by the residue mineralization rates, i.e., SOM decomposition will be dependent on residue type; (ii) regardless of residue type, the intensity of PE will decrease with increasing C addition. We assumed that microorganisms decomposing added residues will represent the most active fraction of soil microflora. Therefore, we further hypothesized that (iii) the PE will be the main function of the soil microorganisms feeding on residues and of its enzyme activities.

Materials and methods

Study area and soil

The soil used for the incubation was sampled from the Ap horizon (0–25 cm) of an experimental field located on a terrace plain of the Leine River northwest of Goettingen, Germany (51° 33′ 36.8″ N, 9° 53′ 46.9″ E). Since more than 25 years, the field has been cultivated with annual C3 crops, predominantly wheat (Kramer et al. 2012). The soil was classified as Luvisol and had a silt-loam texture (6% sand, 87% silt, 7% clay). The pH and a test with 10% hydrochloric acid

indicated the absence of carbonates. The carbonate-free soil had the following characteristics: MB 0.40 ± 0.0 g C kg^{-1} soil, organic C 12.8 ± 0.4 g kg^{-1}; total N 1.3 ± 0.0 g kg^{-1}, pH ($CaCl_2$) 6.0; and $\delta^{13}C$ −26.8‰. After sampling, the soil was air-dried and sieved (<2 mm) and fine roots and other visible crop debris and small stones were carefully removed.

Production of ^{13}C-labeled crop residues

Wheat plants were grown to produce ^{13}C-labeled residues as described in detail by Bromand et al. (2001). Briefly, wheat (*T. aestivum* L.) seeds were grown in pots filled with quartz sand and were watered regularly once a week with Hoagland nutrient solution (N 210, K 235, Ca 200, P 31, S 64, Mg 48 mg l^{-1} plus micronutrients). Following seedling emergence (11 days after seeding), plants were placed inside a transparent closed chamber (120 cm wide × 104 cm high × 60 cm deep) enclosed within a climate-controlled growth cabinet with the following conditions: 16/8-h photoperiod, light intensity at approximately 600 μmol m^{-2} s^{-1}, and mid day and night temperatures of 25 and 15 °C, respectively. The plants were labeled (for at least 8 h) continuously with ^{13}C every week until harvesting. The intended enrichment of CO_2 in the chamber was ~99 atom% ^{13}C. To accomplish this, the CO_2 concentration was first allowed to fall to 327 ppmv in the chamber. Thereafter, ^{13}C-labeled CO_2 was generated by injecting $NaH^{13}CO_3$ (as ~99 atom% $^{13}CO_2$ source) solution through a septum into a generation flask containing 1 M H_2SO_4. The evolved CO_2 was swept into the sealed chamber with a small pump through a closed loop of tubing, and a fan circulated the CO_2 inside the chamber. Wheat plants continued to grow in the chamber until maturity (120 days of growth). Thereafter, the plants were harvested and roots were gently washed to remove the sand particles.

To avoid any preferred decomposition of aboveground and belowground parts of the wheat biomass, plant residues were carefully separated into leaves, stems, and roots. For homogeneous mixing of residues within the soil, each part of the residues was chopped and sieved (2 mm). Carbon and N contents of applied residues varied between residue types, whereby leaves, stems, and roots had C contents of 391.9 ± 6.1 (C/N 17.2 ± 0.3), 409.6 ± 8.7 (C/N 21.5 ± 1.17), and 298.3 ± 5.9 g kg^{-1} (C/N 15.5 ± 0.5), respectively. The atom% ^{13}C values were measured with an isotope ratio spectrometer coupled to an elemental analyzer (Delta plus, EA-IRMS, see detail "Isotopic analysis" section) (Table 1).

Incubation and sampling

For incubation, 50-g soil (dry weight basis) were weighed into 250-ml incubation bottles. The soil was then preincubated (at 22 °C) at 50% water holding capacity (WHC) for 1 week. Thereafter, the 120-day full-factorial incubation experiment with two factors—wheat residue type and residue addition level—was designed. Accordingly, eight treatments were included: three ^{13}C-labeled wheat residue types (leaves, stem, roots), two addition levels (low and high, respectively, 5.4 and 10.8 g dry mass kg^{-1} soil), and one control without residue addition. A reference treatment with the decomposition of crop residues in autoclaved sand was also conducted to consider isotopic fractionation during incubation. All treatments were set with three replicates. The added residues were thoroughly mixed in the soil, and the water contents were then adjusted to 70% WHC. Note, the control soils (without residue addition) also treated in the same way as those with residue addition. The residues were added on a dry matter basis. Accordingly, the C input by roots (with lower C content) corresponds to ca. 70% of the C amount added with leaves or stems.

To estimate MB and enzyme activities, samples were destructively harvested at days 15, 30, 60, and 120 of incubation.

To prove that crop residue was homogeneously labeled, we sampled the partially decomposed residues during the incubation period (destructive sampling). A portion of the incubated soil (ca. 20 g, having residues) was submerged into distilled water; thereafter, the floating material was collected, dried (60 °C), and analyzed for ^{13}C values at IRMS ("Isotopic analysis" section). The isotopic signature of partially decomposed residues revealed that after 2 weeks (intensive residue mineralization), the differences in ^{13}C values for the rest of incubation period did not exceed 0.03 atom% in all treatments (Table 1). This indicated that possible error due to the inhomogeneous (non-uniform) labeling of the residues was minimal and that it did not exceed the variation in ^{13}C between the replicates. The isotopic signature was used as the residue reference material for the mass balance equation.

CO_2 efflux

In order to measure soil respiration, CO_2 was trapped in 5-ml 1-M NaOH trap solution. The trap solution was replaced with fresh 1 M NaOH aliquot at days 2, 4, 7, 11, 23, 30, 36, 46, 60, 81, 101, and 120 of incubation. Therefore, incubation bottles were not closed longer than 21 days and the capacity of NaOH was never used up by more than 60%. An aliquot of sampled NaOH was immediately used to measure total soil and residue-derived CO_2. The total amount of CO_2 trapped in the NaOH solution was determined by titration with 0.05 M HCl against phenolphthalein, after addition of 0.5-M $BaCl_2$ solution.

Microbial biomass

To determine the C content in MB at all destructive sampling periods, the chloroform fumigation-extraction method was used as already described by Makarov et al. (2015) and

Table 1 The ^{13}C values (atom%) of leaves, stems, and roots of wheat residues at different decomposition stages over the incubation period at days 0, 15, 30, 60, and 120

Residue type	0 day	15 days	30 days	60 days	120 days
Leaves (^{13}C atom%)	1.54 (0.00)	1.41 (0.01)	1.43 (0.00)	1.40 (0.02)	1.41 (0.01)
Stems (^{13}C atom%)	1.36 (0.00)	1.32 (0.00)	1.33 (0.00)	1.31 (0.00)	1.31 (0.01)
Roots (^{13}C atom%)	1.51 (0.00)	1.46 (0.00)	1.47 (0.01)	1.40 (0.04)	1.45 (0.01)

Numbers in brackets: ±SE of mean

Vance et al. (1987). Briefly, 6-g (moist) soil was extracted with 24 ml of 0.05 M K_2SO_4 for 1 h. The other 6-g soil were firstly fumigated with ethanol-free $CHCl_3$ for 24 h at 22 °C and then extracted in the same way. The obtained extracts were analyzed for total C content using a TOC/TIC analyzer (Multi N/C 2100, Analytik Jena, Germany). The MB-C (K_2SO_4 extractable) was calculated as E_C/K_{EC}, where E_C is the difference between extracted organic C of fumigated and non-fumigated soils and K_{EC} = 0.45 (Wu et al. 1990).

Enzyme assays

The enzyme activities at all sampling periods (15, 30, 60, and 120 days) were measured using fluorogenically labeled substrates (Pritsch et al. 2004; Sanaullah et al. 2016). Five fluorogenic enzyme substrates based on 5-methylumbelliferone (MUF) were used: MUF-β-D-cellobiohydrolase (MUF-C; EC 3.2.1) for cellobiohydrolase, MUF-β-D-xylopyranoside (MUF-C; EC 3.2.1) for xylanase, MUF-*N*-acetyl-β-D-glucosaminide dehydrate (MUF-NAG; EC 3.2.1.14) for chitinase, MUF-β-D-glucopyranoside (MUF-G; EC 3.2.1.21) for β-glucosidase, and MUF-phosphate monoester (EC 3.1.3.2) for acid phosphomonoesterase (Nannipieri et al. 2011). L-Leucine-7-amino-4-methylcoumarin (AMC) substrate was used to estimate L-leucine aminopeptidase (LAP) activity. All enzyme substrates were purchased from Sigma (Germany).

Briefly, 0.5 g of soil (dry weight basis) was dispersed in 50 ml of deionized water for 2 min using low-energy sonication (40 J $_S^{-1}$). Then, 50 μl of the suspension was pipetted into 150-μl specific enzyme substrate solution (containing 50 μl of MES or Trizma buffer for MUF or AMC substrates, respectively) having a final concentration of 200 μmol g^{-1} soil. Fluorescence was measured by incubations of soil suspension (for 2 h at 22 °C) in 96-well microplates (Puregrade, Germany) with fluorogenic substrates at an excitation wavelength of 355 nm and an emission wavelength of 460 nm and slit width of 25 nm, with a Victor R^3 1420 Multilabel Counter (PerkinElmer, Waltham USA).

Isotopic analysis

Since we used ^{13}C-enriched plant material, the CO_2-trapped NaOH samples were specifically prepared for isotopic analysis. For this, 3 ml of CO_2-trapped NaOH solution was precipitated with an equal volume of 1-M $SrCl_2$ solution. The NaOH solution containing $SrCO_3$ precipitates was then centrifuged for 5 min at 2680×*g*. The process was repeated with distilled water to remove excess NaOH and to reduce pH to 7. After removing water, $SrCO_3$ pellets were dried at 60 °C and stored for ^{13}C analysis by an isotope ratio mass spectrometer (Delta plus, IRMS; Thermo Fisher Scientific, Bremen, Germany). The ^{13}C values were expressed as atom%. The estimations were calibrated with reference to the international Vienna Peedee Belemnite (VPDB) standard. For ^{13}C measurement of MB, an aliquot (ca. 10 ml) of the K_2SO_4 extract was freeze-dried, and thereof, solid material was analyzed.

Calculations

To partition residue- and SOM-derived C in total CO_2 and microbial C, calculations were done step by step as suggested earlier (Blagodatskaya et al. 2011a; Poirier et al. 2013).

Firstly, the ^{13}C values ($atom_{\%}$) were calculated according to the following equation.

$$\text{Atom\% } {}^{13}\text{C} = \left[\text{number of } {}^{13}\text{C atoms}/\text{number of } \left({}^{12}\text{C}+{}^{13}\text{C}\right)\text{atoms}\right] \cdot 100 \quad (1)$$

Then, the fraction of residue-derived C ($f{\cdot}C_{res}$) was calculated according to the mass balance equation (Hayes 2004):

$$f \cdot C_{res} = (At_{mix}\text{-}At_{con})/(At_{res}\text{-}At_{con}) \quad (2)$$

where At_{mix} represents ^{13}C atom% values of the residue-amended soil evolved as CO_2 (trapped in NaOH) or present in fumigated or non-fumigated K_2SO_4 extracts. At_{res} represents specific ^{13}C atom% values of the corresponding residue source (i.e., leaves, stems, roots). At_{con} shows ^{13}C atom% values of each corresponding pool of soil without residue addition.

Finally, the amount of residue-derived C (C_{res}, g kg^{-1}) was calculated according to Eq. (3):

$$C_{res} = f \cdot C_{res} \cdot [TC] \quad (3)$$

where [TC] represents the total C amount of the corresponding pool (i.e., CO_2, fumigated, and non-fumigated K_2SO_4 extracts)

The amount of SOM-derived C (C_{SOM}, g kg^{-1}) was simply calculated by subtracting C_{res} from the total C of the corresponding pool.

The amount of primed C released as total CO_2, i.e., PE (g C kg^{-1}), was calculated according to the following equation.

$$PE = CO_2 \cdot C_{total} - CO_2 \cdot C_{res} - CO_2 \cdot C_{control} \quad (4)$$

To estimate the residue-derived C fraction present as MB (Res_C_{MB}) in each destructive sampling and at the end of incubation, firstly, residue-derived C was calculated separately for fumigated and non-fumigated samples using Eq. 3. Then, calculations were done according to the following equation.

$$Res\_C_{MB} = (f \cdot C_{res} - nf \cdot C_{res}) \Big/ (f \cdot C - nf \cdot C) \quad (5)$$

where $f{\cdot}C_{res}$ and $nf{\cdot}C_{res}$ are the C_{res} values of fumigated and non-fumigated samples, respectively, calculated according to Eq. 3. $f{\cdot}C$ and $nf{\cdot}C$ are the amounts of total C in fumigated and non-fumigated samples, respectively, determined as discussed in "Microbial biomass" section.

The relationship of both CO_2 efflux and enzyme activities was highly positively correlated with the Res_C_{MB} instead of total MB-C. Therefore, to estimate specific PE and enzyme activities (in relation to Res_C_{MB}), the absolute amounts of PE (calculated according to Eq. 4) and enzyme activities (as described in "Enzyme assays" section) were divided by the total amounts of Res_C_{MB}, which was calculated according to Eq. 5.

Threshold values for PE increase

The relationship between the fraction of mineralized residue, x (as % of initial input), and specific priming effect (PE) was best explained and fitted by a unifying model (combining logistic and power functions):

$$PE(x) = a \cdot x^2 + b \Big/ [1 + \exp(-c \cdot (x - d))] + e \quad (6)$$

where $PE(x)$ represents the specific PE, x the value of mineralized fraction of crop residues, a the residue quality coefficient, b the maximal PE value, c the residue-specific maximal rate of PE increment, d the mineralized fraction of residues at maximal rate of PE increment, and e the minimal PE value. Model parameters were optimized for best fitting of the model output to experimental data. All fits were done with Excel Solver facilities. For all the types of crop residues, the model demonstrated an excellent goodness of fit with r^2 above 0.98. The model enabled estimation of the threshold value of the mineralized fraction of crop residues when maximal changes in PE increment occur. That corresponds to the point where the second derivative of the function (6) has its maximum.

Statistical analysis

The experiment was carried out as a full-factorial, completely randomized design. The factor "type" had three levels (leaves, stems, roots) and the factor "addition" had two or three levels (no, low, and high addition). Time was considered as a random factor where applicable. Two addition levels were used when comparing residue-derived C where inclusion of "no addition" was not suitable. Statistical analyses were performed with SPSS 11 using a two-way ANOVA (when the time was not considered) and three-way ANOVA with "addition level," "type" as fixed effects, and "time" as a random effect. When significant ($p \leq 0.05$) effects were found, post hoc comparisons of means were performed using Fisher's least significant difference test (Webster 2007). The error propagation was calculated when the mean values were used for determining PE (Meyer 1975). Correlations (r) between MB (derived from residue and SOM) values and CO_2 or potential enzyme activities in soils were analyzed by Pearson's correlation method.

Results

^{13}C in crop residues during incubation

The ^{13}C values of incorporated residues were specific to residue type; i.e., leaves, stem, and root had 1.54, 1.36, and 1.51 ^{13}C atom%, respectively. During the incubation period, the ^{13}C values of partially decomposed residues mainly declined until day 15 and thereafter remained nearly constant for the rest of incubation period, indicating that residues were homogeneously labeled (Table 1). The averaged (±SD) ^{13}C (atom%) values of partially decomposed residues of leaves, stem, and roots across all sampling period were 1.41 ± 0.01, 1.32 ± 0.01, and 1.44 ± 0.03, respectively (see "Incubation and sampling" section). Accordingly, very similar ^{13}C values of the CO_2 evolved from reference treatments with sand were detected. The average (±SD) values of ^{13}C (atom%) across sampling periods were 1.41 ± 0.03, 1.30 ± 0.02, and 1.42 ± 0.01 for leaves, stems, and roots, respectively.

Residue and soil organic matter mineralization

Residue addition caused a significant increase in total soil CO_2 efflux compared to the control without additions. At low additions, the amount of total CO_2 efflux was higher in leaves and stems (for both, up to 1.9 g C kg^{-1}) than in roots (1.5 g C kg^{-1}) (Fig. S1 Supplementary Material). At the high residue addition level, absolute CO_2 efflux also increased. Similar to low additions, no differences in total efflux between leaves and stems (3.3 g C kg^{-1}) were also found at high additions.

The total amount of SOM-mineralized C in the control was 0.65 g C kg^{-1} soil over 120 days of incubation. Mineralization of SOM significantly increased with residue addition depending on the type and amount of residue (Fig. 1a). At the doubled amount of residue addition, the cumulative SOM mineralization remained similar between low and high addition levels of leaves (up to 0.9 g C kg^{-1}) and stems (1.1 g C kg^{-1}). In contrast, SOM mineralization under high root addition increased up to 15% compared with low additions (Fig. 1a).

The residue mineralization rate was significantly affected by both type and level of additions. Total mineralization was highest in leaves and lowest in roots (Fig. 1b). Depending on the quality and on the added amount, two distinct residue mineralization phases (intensive and slow) were observed. Remarkably, during the intensive phase, the residue decomposition was proportional to the added amount (for leaves and stems, ca. 2–3 weeks) (Fig. 1b). During the slow phase (after 2–3 weeks), residue mineralization was disproportionally stronger for high versus the low amount of leaves and stems, but not for roots.

Therefore, at the end of the experiment, at low addition, the leaf-, stem-, and root-derived CO_2 reached 1.0, 0.9, and 0.4 g C kg^{-1}, corresponding to 46, 38, and 29% of their initial additions, respectively (Fig. 1b). Relative root mineralization after intensive phase was similar at high and low addition (i.e., 29% of initial input), whereas the leaf and stem mineralization rate were up to 17 and 30% faster at high than at low additions, respectively (Fig. 1b).

Priming effect

A significant increase in the SOM-originated CO_2 efflux after residue addition caused a positive PE, but the PE intensity was strongly affected by residue quality and amount (Fig. 1c). The maximum PE was recorded for root (increase with the addition level 0.42 to 0.58 g C kg^{-1}) and lowest (even negative) for leaf addition (0.20 to 0.27 g C kg^{-1}). Remarkably, larger PE was observed at low versus the high amount of stems and leaves during the intensive phase of decomposition. Furthermore, the cumulative PE remained negative under high leaf addition during the initial ca. 6 weeks of incubation (Fig. 1c).

As the added residues varied in their C contents (see "Production of ^{13}C-labeled crop residues" section), the specific PE was calculated based on C addition (Fig. 1d). The amount of specific PE (per unit of C) in root treatments was significantly higher than that of leaves and stems at both

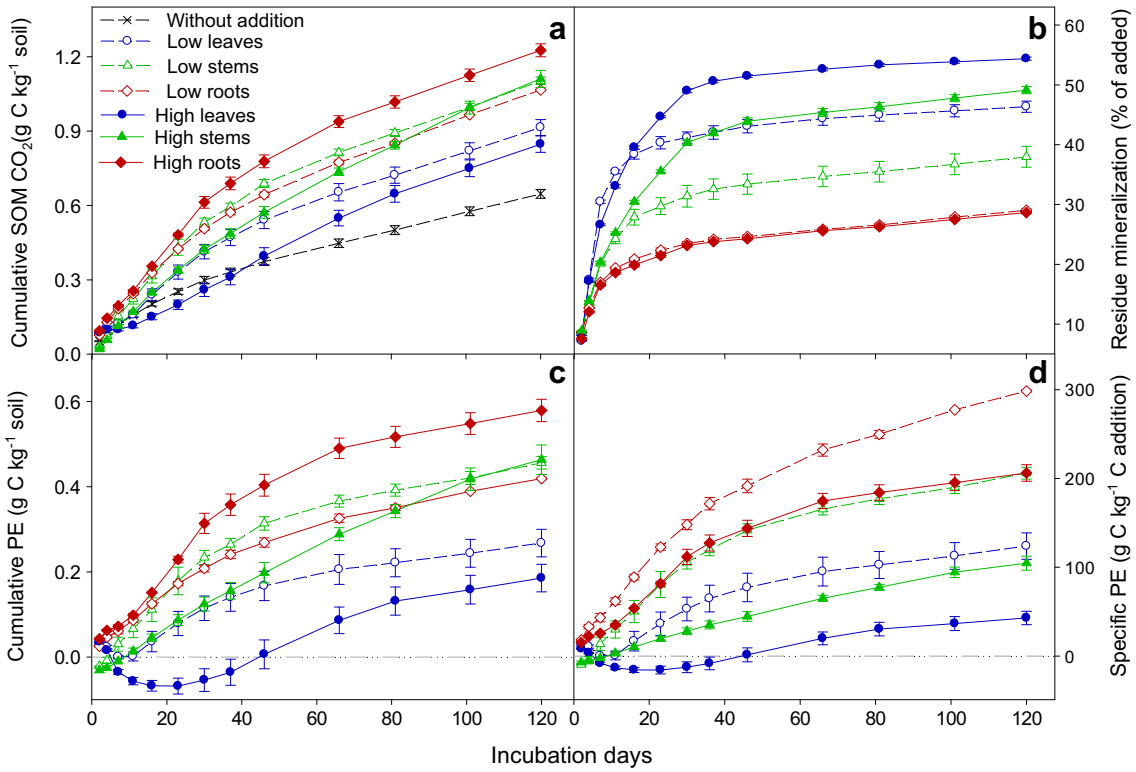

Fig. 1 Cumulative CO_2 release originated from soil organic matter (SOM, **a**), crop residue decomposition (% of initial addition, **b**), total priming effect (PE, **c**), and specific PE (**d**) over 120 days of incubation, depending on the residue type and addition level. Mean values with standard errors (n = 3). The p values of the ANOVA showing the effect of different factors for all; cumulative CO_2 release originated from SOM (**a**), residue decomposition (% of initial addition, **b**), total PE (**c**), and specific PE (**d**) are as follows: type <0.001, level <0.001, and their interactions: level × type <0.001

residue addition levels (Fig. 1d). The total amounts of specific PE in root treatments were 300 and 200 g C kg^{-1} at low and high root C addition, respectively.

Regardless of residue type, specific PE decreased at high versus low C addition (Fig. 1d), suggesting that the PE depended on the amount of decomposed residues. To clarify this relationship, we plotted the cumulative specific PE against residue-originated CO_2 (Fig. 2). After a lag period, the PE increased strongly over the course of residue decomposition. This demonstrates that during the initial intensive phase, the decomposition rate of residues exceeded the PE. During the slow phase of residue decomposition, however, the PE increased drastically. A threshold (calculated by the second derivative, see "Threshold values for PE increase" section) of the decomposition function indicated that such a drastic increase in PE occurred when ca. 20, 29–44, and 39–51% of (low and high) roots, stems, and leaves were decomposed, respectively (Fig. 2).

To differentiate the contribution of various sources of CO_2 efflux from soil (within residue additions), respired from soil over 120 days, total respiration was partitioned (% contribution) into basal respiration, residue originated, and PE (Fig. 3). The basal respiration (from the control 0.65 g C kg^{-1}) was assumed to be constant for all residue additions. At the end of the experiment, 53–73, 43–66, and 28–40% of added leaves-, stems-, and roots-originated CO_2 contributed to their corresponding total CO_2 efflux. At high addition, the percentage of primed C in total CO_2 efflux was lower in the leaves and stems versus their low addition level. At high additions, root-induced primed C percentage of total respiration remained the same as at its low addition levels, but the contribution of basal respiration was reduced, which was substituted by residue-originated C (Fig. 3).

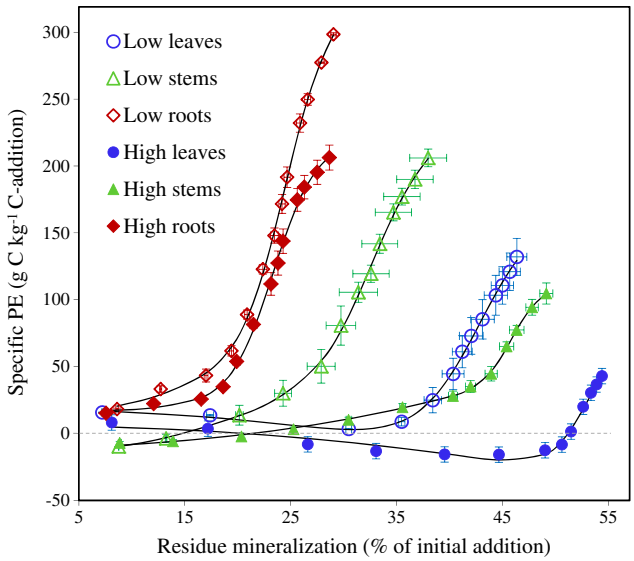

Fig. 2 The relationship between the fraction of mineralized residue, x (as % of initial input), and soil-specific priming effect (PE) was best explained and fitted by a unifying model (combined with logistic and power functions): $PE(x) = a \cdot x^2 + b/[1 + \exp(-c \cdot (x - d))] + e$. Means and standard error ($n = 3$)

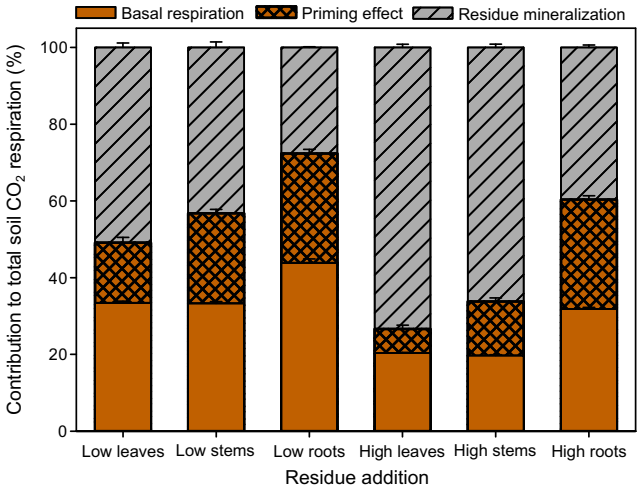

Fig. 3 The relative contribution (%) of carbon (C) sources from basal respiration, priming effect, and residue mineralization to their corresponding total soil CO_2 efflux after 120 days of incubation, depending on the residue type and addition level. Basal respiration (without addition) was assumed to be constant for all residue-treated soils. Means and standard errors ($n = 3$). The p values from the ANOVA showing the factor effect are as follows: basal respiration (type <0.001, level <0.001, and their interactions: type × level = 0.081) and for both priming effect and residue mineralization are as (type <0.001, level <0.001, and their interactions: type × level <0.001)

Microbial biomass

Consistent with the CO_2 efflux, adding residues significantly (28–85%) increased MB-C compared with control. This highlights the microbial demands for C and nutrients. The MB-C significantly increased (compared to the control) during the intensive decomposition phase of the residues (during the first 2 weeks), with an average of 42–85, 42–53, and 28–54% due to leaf, stem, and root addition, respectively (Fig. 4a). Remarkably, the increase of MB-C was solely (intensive phase) or mainly (slow phase) due to residue-feeding microorganisms, because the differences in SOM-decomposed biomass were insignificant (except at day 120). The amount of residue-derived C present as MB (Res_C_{MB}) was the highest under leaves (0.07 to 0.37 g C kg^{-1} soil) and the lowest under root additions (0.02–0.17 g C kg^{-1} soil) across all sampling periods (Fig. 4a). Despite a major overall drop (15–60 days) in biomass during the slow decomposition phase, the MB in residue-treated soil still remained higher than in the control (exception: low root treatment at days 30 and 60). This again was mainly due to residue-decomposing microorganisms. Remarkably, the percentage of SOM-derived C in MB in all residue treatments exceeded the control, only at day 120 indicating a relative increase of SOM-C incorporation in MB. A

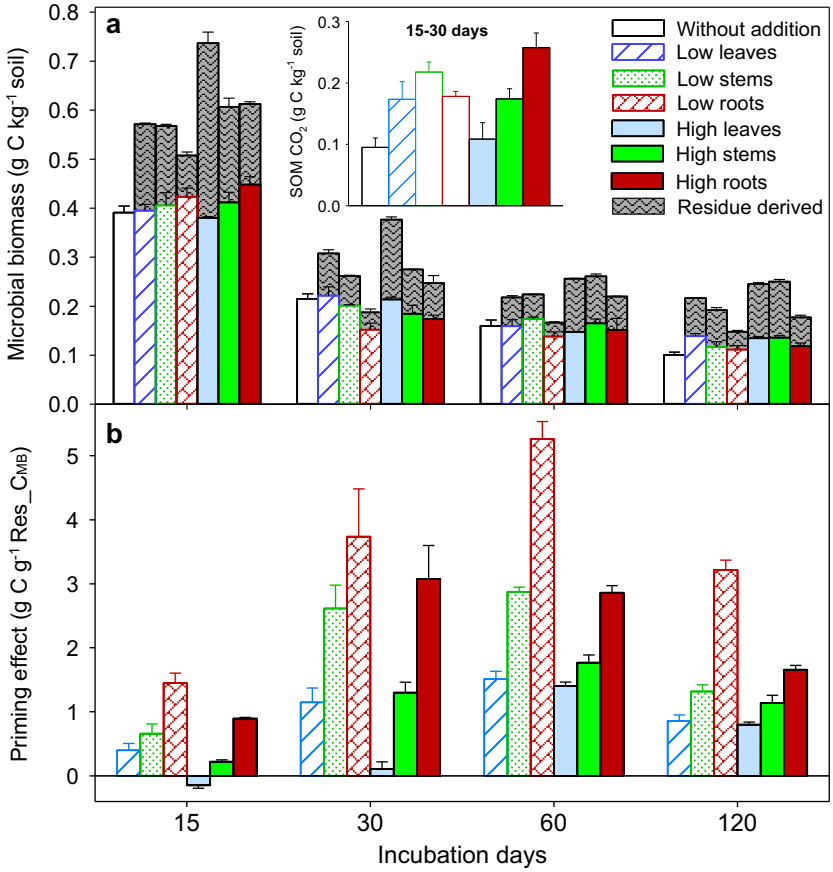

Fig. 4 The contribution of soil organic matter (SOM) and crop residues originated C (Res_C_{MB}) to total microbial biomass (**a**) and the amount of priming effect per unit of Res_C_{MB} (**b**), depending on the residue type, addition level, and time of sampling. The *inset* (**a**) shows the amount of total SOM-derived CO_2 during the period of 15–30 days. Means with standard errors ($n = 3$). The *p*-values from the ANOVA showing the factor effect on SOM originated microbial biomass (type = 0.043, level = 0.174, time <0.001, type × level = 0.042, type × time <0.001, level × time = 0.661, and level × type × time = 0.546) and on Res_C_{MB} (for all factors, i.e., type, level, time, and their interactions, $p < 0.001$). Similarly, *p* values for priming effect per unit Res_C_{MB} (b) are as, for all factors and interactions, ≤0.001 (except the interaction of type × time, $p = 0.307$)

stronger positive correlation between ^{13}C-labeled MB (Res_C_{MB}) than SOM was found with total CO_2 and residue-originated CO_2 effluxes, at all sampling periods (Table S1, Supplementary Material). Similarly to specific PE, the PE calculated per unit of Res_C_{MB} was greater at low than at high residue addition (Fig. 4b). At both addition levels, the PE per unit Res_C_{MB} from roots was significantly higher than that of leaves and stems.

Enzyme activities

The activities of all tested enzymes increased significantly after residue addition. Enzyme activity highly depended on residue type and the amount of addition (generally increasing with addition level) and sampling time (Fig. S2, Supplementary Material). The correlation between enzyme activity and MB-C was relatively weak, but it was highly strengthened when it correlated with ^{13}C MB-C (Res_C_{MB}) (Table 2, Supplementary Material). The correlation between enzyme activity and SOM-derived MB was mainly negative or insignificant. Therefore, enzyme activities are presented as specific activity per unit of Res_C_{MB} (Fig. 5).

Overall, the specific enzyme activities (nmol μg^{-1} Res_C_{MB} h^{-1}) were lowest on incubation day 15 (Fig. 5). At both addition levels, the activities involved in the C-cycle (β-glucosidase, β-cellobiohydrolase, chitinase, xylanase) remained stable. The acid phosphomonoesterase and leucine aminopeptidase activity increased until day 60 and then decreased again (Fig. 5). Enzyme-specific activity was significantly higher under root than under both leaf and stem addition at all sampling periods. With the increase of residue addition level, however, the specific activity significantly decreased compared with low residue addition (Fig. 5). No significant differences in enzyme activities between leaf and stem additions were observed at both addition levels. The positive correlation between the specific PE and enzyme activities consistently increased with the increased specific PE and was the strongest for β-glucosidase, acid phosphomonoesterase, and leucine aminopeptidase activity (Table 2).

Discussion

Residue and soil organic matter decomposition

Residue quality effects

Our first hypothesis (i.e., SOM decomposition dependence on residue type) was confirmed by the simultaneous but inverse intensity of CO_2 efflux originating from SOM and from crop

Table 2 The Pearson correlations (r) between specific priming effect and values of specific enzyme activities at days 15, 30, 60, and 120 of incubation in soils amended with residues

	β-Glucosidase	Acid phosphatase	Chitinase	Xylanase	Cellubiosidase	LAP
15 days	0.74	0.61	-0.19	0.43	0.27	0.71
30 days	0.69	0.78	0.66	0.66	0.40	0.67
60 days	0.82	0.80	0.64	0.69	0.68	0.82
120 days	0.90	0.82	0.77	0.72	0.74	0.81

LAP leucine aminopeptidase

residues. SOM decomposition was very low during the intensive phase of residue mineralization (up to 3 weeks) and thereafter increased when residue mineralization rate declined. Roots had a lower and shorter intensive mineralization phase than leaves and stems, but relatively intensive SOM decomposition indicated high SOM vulnerability (Chen et al. 2015; Shahbaz et al. 2016a). Note, however, that a twofold increase of residue addition triggered an up to 2.3 and 2.6 times higher mineralization of leaves and stems, whereas SOM decomposition remained unaffected. This demonstrated that high rates of residue mineralization reflect great substrate C availability, which did not cause an increase in SOM decomposition. Microorganisms preferably utilize substrates if their availability is high, and therefore, SOM decomposition is not necessarily to be increased (Nottingham et al. 2009; Wang et al. 2015). In contrast to this, SOM decomposition was substantially increased (up to 15%) at the doubled amount of root additions. This proved the high susceptibility of SOM to decomposition in the presence of decaying roots (Shahbaz et al. 2016a). Despite roots were characterized by the C/N ratio close to leaves, the roots were least decomposed. This can be attributed to the biochemical composition: root contains relatively less readily decomposable compounds and high amount of recalcitrant substances such as lignin, suberin, phenols, and tannin (Aber and Melillo 1982; Bertrand et al. 2006; Lian et al. 2016; Rasse et al. 2005). Soil microorganisms feeding on such slowly decomposable substances produce enzymes able to degrade similar compounds in SOM via cometabolism (Horvath 1972; Kuzyakov et al. 2000). Here, we extend the meaning of cometabolism assuming that microorganisms producing such enzymes can also utilize SOM decomposition products.

Priming effect as a function of residue mineralization threshold levels

The occurrence of PE after residue incorporation suggests that substrate addition (C availability) changed microbial stoichiometry that accelerated SOM decomposition for balanced microbial growth (Chen et al. 2014). This explains, in accordance with the priming conceptual models, the development of PE due to microbial C limitation (Blagodatskaya and Kuzyakov 2008). Here, we further developed a concept on the PE dynamics as depending on the quality and quantity of crop residues.

In accordance with our second hypothesis, specific PE (per unit of residue C) was lower at high than at low residue additions. Such decrease in PE mostly occurs when the abundant amount of easily decomposable substrate is available (Guenet et al. 2010). This is often explained by the microbial substrate C saturation and their preferential substrate utilization over SOM (Blagodatskaya and Kuzyakov 2008; Xiao et al. 2015). The decrease of PE at high C additions highlights the relation of PE with residue decomposition (Wang et al. 2015). The PE was lowest during the intensive phase of residue mineralization and thereafter increased strongly. According to a unifying model (logistic and power functions), a threshold of ca. 20, 29–44, and 39–51% mineralization of roots, stems, and leaves, respectively, exhibited the strong increase of PE at the slow residue decomposition phase (Fig. 2). This showed that the onset of strong priming growth was up to 2.5 times faster (earlier) under root additions compared with leaf and stem additions. Accordingly, at high crop residue addition, the start of strong increase of PE was delayed by a factor of up to 1.5 for both leaves and stems (exhibiting quantity effect) versus not for roots. This residue decomposition and PE phenomena (depending on quality and quantity of input) indicated a changing microbial substrate utilization pattern (Nguyen and Marschner 2016; Wang et al. 2015), which may result in a variable amount of apparent and real PE (Garcia-Pausas and Paterson 2011; Blagodatskaya et al. 2014).

Mechanisms of priming effect

Apparent and real priming effect in relation to residue mineralization

The mechanisms of PE relate the extra-CO_2 emission with the sources of the primed organic matter. During the intensive residue mineralization phase: the low or even negative PE suggested a preferential substrate utilization (or pool substitution) mechanism mainly for leaves (ca. 2–3 weeks) and stems (Blagodatskaya and Kuzyakov 2008; Fontaine et al. 2003). Importantly, this phase lasted much longer for leaf and stem additions than for the roots, showing apparent PE (Figs. 2 and 6) (Paterson and Sim 2013). Afterward (15–60 days), the increase in primed CO_2 was accompanied by up to 60%

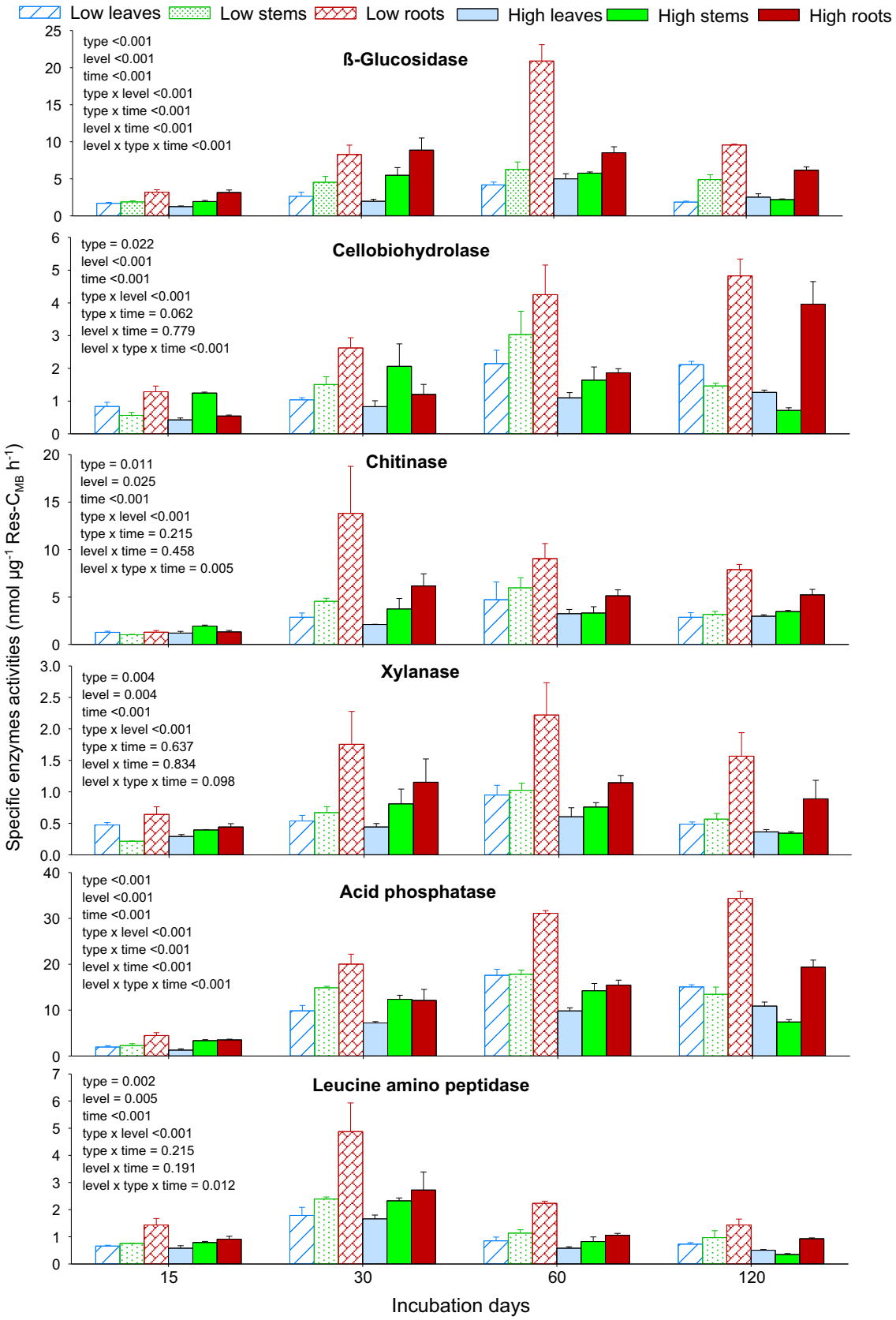

Fig. 5 Specific enzyme activities (enzyme activities per unit of residue originated microbial biomass (Res_C_{MB})), depending on the residue type, addition level, and time of incubation. Mean values with standard errors ($n = 3$). The presented p values are from the ANOVA of the data (residue type, addition level, time of sampling, and their interactions)

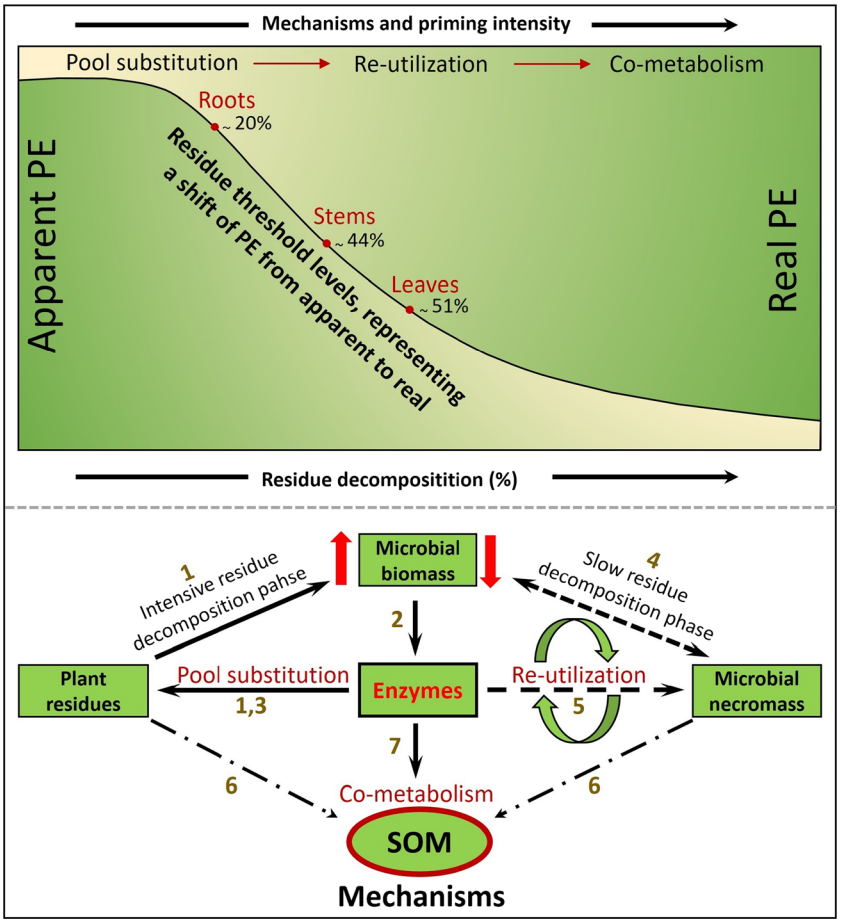

Fig. 6 Conceptual scheme of apparent and real priming effect (PE) in soil after residue addition, explained by three main mechanisms: pool substitution, reutilization, and cometabolism. Residue mineralization threshold levels, as estimated by a unifying model (logistic plus power functions), represent the shifts of PE from apparent to real when ca. 20% (roots), 44% (stems), and 51% (leaves) of added residues (i.e., at high additions) were mineralized. Mechanisms: *1*—microbial uptake of plant residues degraded by existing enzymes leads to initial increase of microbial (active) biomass (MB), which is mainly due to the residue-feeding population; *2*—acceleration in enzyme production after residue-induced increase in MB (depending upon residue type); *3*—preferential substrate utilization (under high substrate C availability) leading to pool substitution mechanism (1, 2, 3); *4*—decrease of MB during slow residue decomposition phase (after exhaustion of labile substrate), which results in the accumulation of microbial necromass, i.e., after microbial starvation and cell death; *5*—reutilization (2,4,5) of microbial necromass under low substrate availability; *6*—direct contribution of microbial necromass and plant compounds in soil organic matter (SOM) formation; and *7*—increase of enzymatic SOM decomposition by cometabolism under low availability of labile crop residue compounds (depending on residue quality)

decrease in MB and by increased specific enzyme activities (compared with at day 15). Surprisingly, no incorporation of SOM-derived C into MB was detected during this period. This suggested an occurrence of a new mechanism of real PE primarily from reutilization of microbial necromass (produced after a strong decrease in MB), indicating that necromass served as SOM primer (Fig. 6) (Miltner et al., 2009, 2012). At a later stage, the PE strongly exceeded residue decomposition and it was accompanied by incorporation of SOM-derived C into MB. This indicated an occurrence of real PE, possibly due to microbial shifts, i.e., from fast- to slow-growing (e.g., fungi) SOM-feeding populations (Blagodatsky et al. 2010; Nannipieri et al. 1978). This phase of PE was much faster (started earlier) and stronger under root versus leaf and stem addition (Figs. 2 and 6). Therefore, the sequence of PE mechanisms was more complex during decomposition of aboveground crop residues compared with roots.

Priming effect mechanisms in relation to microbial biomass and enzyme activities

The lower amount of root- than leaf- or stem-originated C in MB confirms that root C was relatively less labile and its decomposition was slower (Cotrufo et al. 2013; Stewart et al. 2015). The MB peaked due to residue additions at day 15, without an increase in SOM-originated C compared to the control. The correlation between the PE and enzyme activity was relatively weak in that period. We, therefore, interpret the PE occurring during the intensive decomposition phase as apparent, mainly due to the pool substitution (or preferential

use) mechanism (Blagodatskaya and Kuzyakov 2008; Garcia-Pausas and Paterson 2011). The fast decline of MB demonstrates the exhaustion of the labile portion of residue and SOM-originated C, which is often observed in other studies (Blagodatskaya et al. 2011b; Wang et al. 2016). The decline of MB during 15–30 days, e.g., by ca. 0.2 g C kg^{-1} in the without addition control was confirmed by at least 0.1 g C kg^{-1} of SOM-derived CO_2-C emissions during that period (Fig. 4a). Similar pattern was observed in the residue-treated soils where SOM-derived CO_2-C emission corresponded well to the decline in SOM-originated microbial C. Such PE can already be considered as real assuming extra CO_2 originated from the labile SOM-fraction (i.e., microbial necromass) and that the PE was accompanied by increased enzyme activity (Blagodatskaya and Kuzyakov 2008; Miltner et al. 2009; Paterson and Sim 2013). The specific PE and enzyme activities mainly correlated with residue-metabolizing MB, indicating the link of the residue-feeding microbial fraction to PE. Remarkably, this PE mechanism has never been before experimentally demonstrated. The significant increase of SOM-derived C in MB after 120 days corresponded to the strong correlation between the PE and enzyme activity (Fig. 4a and Table 2). This suggests that the possible mechanism of real PE was due to the cometabolism of recalcitrant SOM during the decomposition of less labile crop residues.

Residue addition enhanced microbial activity, boosting enzyme production (Fig. S2, Supplementary Material) (Blagodatskaya and Kuzyakov 2013; Fontaine et al. 2003). Due to stronger positive correlations, the residue-originated (Res_C_{MB}) rather than the SOM-originated soil microflora appeared to be mainly responsible for decompositions and enzyme activities (Table S1, Supplementary Material), further supporting our third hypothesis.

Residue addition stimulated specific activities (per unit of Res_C_{MB}) of all six tested enzymes (Fig. 5). The decrease of specific enzyme activities at high residue additions can be due to the decreasing rate of enzyme production because of lower energy demands (microbial saturation by substrate) (Xiao et al. 2015). The increase of these activities after the intensive phase of residue decomposition confirms that microorganisms were at a nutrient limitation, or starving stage, causing (real) PE (Blagodatskaya et al. 2014). Accordingly, a strong interaction between specific enzyme activities and PE further supported microbial necromass reutilization mechanism, i.e., a real PE.

At both addition levels, higher root-induced specific PE and enzyme activities than leaves and stems may be due to the complex root structure (less decomposability) and low C availability. Thus, microorganisms synthesized more enzymes able to hydrolyze root components as well as similar compounds from SOM. This caused real PE based on cometabolism (Kuzyakov et al. 2000; Paterson and Sim 2013). Although residue-originated C in MB under root additions was lowered compared with leaves and stems, microorganisms involved in root degradation produced enzymes (specific activity): probably, this community was more efficient due to substrate quality (Fig. 5). Our study emphasizes the role of crop residue-feeding microorganisms as active players explaining the mechanisms and thresholds of PE, which are induced by contrasting crop residue quality and quantity.

Overall, we summarize that the partitioning of C sources (residue and primed) during residue decomposition is combined with residue-originated MB and specific enzyme activity (Figs. 4 and 5). The results demonstrated that instead of the total MB, the crop residue-feeding microorganisms served as the main player regulating PE mechanisms, which depended on residue mineralization stage (threshold levels). Residue quality and amount strongly influenced the MB and microbial activity (high MB under leaf, low under root additions) involved in crop residue and SOM decomposition (Fig. 6) (Blagodatskaya et al. 2014). The increase in MB after residue addition was mainly due to crop residue-feeding microbial fraction. During intensive phase, crop residues preferably decomposed due to accelerated enzyme production (specific), which mainly correlated with the residue-feeding microbial population. This caused apparent PE by a pool substitution (roots and stems) and negative PE by preferential residue decomposition mechanisms (Fig. 1d, stages 1, 2, and 3 in Fig. 6). Later, a strong decrease in MB (resulted in an increase of microbial necromass) and a high correlation of enzyme activity with PE occurred. This indicated real PE induced primarily by the reutilization of microbial necromass (stages 2, 4, and 5 in Fig. 6, Miltner et al. 2012). Subsequently, cometabolism of recalcitrant SOM was seen when an increase in SOM-originated C in MB was accompanied by an increase in specific enzyme activities. The specific enzyme activity strongly depends on crop residue C availability: unless the decomposability or C availability is high, microorganisms will produce less enzymes capable to cometabolize SOM and there will be a less need for reutilization of microbial necromass (resulting in low or negative PE). Under low residue decomposability, i.e., less C availability (e.g., roots), microbial dynamics yield only a brief pool substitution stage. Nonetheless, reutilization and cometabolism will be the dominating processes, creating real PE (Fig. 6).

Conclusions

Root residues induce faster and stronger PE than aboveground plant parts. For all residue types, specific PE (per unit of C addition) decreased with added residue amounts. The slow root decomposition leads to stronger PE. The leaf and stem residues were intensively mineralized and yielded negative or

apparent PE for extended periods, due to preferential utilization and pool substitution mechanisms. This resulted in a shorter real PE compared to root addition. During the 15–60 days, the MB declined strongly but specific enzyme activities increased. Remarkably, no incorporation of SOM-derived C into MB was detected during up to 60 days. Therefore, this suggests that the PE was primarily caused by reutilization of microbial necromass; i.e., necromass served as SOM primer. At the end of incubation, the incorporation of SOM-originated C into MB and a corresponding increase in enzyme activities indicated the cometabolism of SOM. The amount of primed SOM correlated with the residue-feeding microorganisms and depended on residue decomposition phases, residue quality. and the added amounts. This underlines the role of residue-feeding microbial community as an active player for PE that is responsible for the contrasting PE mechanisms. We recorded threshold levels for the onset of strong PE increase versus the fraction of mineralized residues at ca. 20, 29–44, and 39–51% mineralization of low and high input of root, stem, and leaves, respectively. We conclude that for microbially mediated SOM decomposition, the residue mineralization stage is crucial, which depends not only on the quality but also on the quantity of added residues. Further research efforts should focus on evaluating the role of microbial necromass in stable SOM formation and PE under contrasting substrate quality and on utilizing enzyme assays (e.g., for oxidative enzymes) to assess the recalcitrance of newly formed SOM compounds.

Acknowledgements We acknowledge the financial support provided by the German Academic Exchange Service (DAAD) to MS and Alexander von Humboldt Foundation (AvH) to MSU. EB's participation was supported by the Russian Science Foundation (project N 14-14-00625). We also acknowledge the technical support of Klaus Schützenmeister in isotope labeling of the plant material. We are thankful to Karin Schmidt and Anita Kriegel for laboratory assistance. The isotopic analyses were performed at the Kompetenzzentrum Stabile Isotope (KOSI), Goettingen. This study was funded by the Deutsche Forschungsgemeinschaft (DFG, projects HE 6726/6 and KU 1184/29).

References

Aber JD, Melillo JM (1982) Nitrogen immobilization in decaying hardwood leaf litter as a function of initial nitrogen and lignin content. Can J Bot 60:2263–2269. doi:10.1139/b82-277

Adair EC, Parton WJ, Del Grosso SJ, Silver WL, Harmon ME, Hall SA, Burke IC, Hart SC (2008) Simple three-pool model accurately describes patterns of long-term litter decomposition in diverse climates. Glob Chang Biol 14:2636–2660. doi:10.1111/j.1365-2486.2008.01674.x

Berg B, McClaugherty C (2014) Decomposition as a process: some main features. In: Berg B, McClaugherty C (eds) Plant litter — decomposition, humus formation, carbon sequestration, Third Edition Edn. Springer, Heidelberg, New York, Dordrecht, London, pp. 11–34. doi:10.1007/978-3-642-38821-7_2

Bertrand I, Chabbert B, Kurek B, Recous S (2006) Can the biochemical features and histology of wheat residues explain their decomposition in soil? Plant Soil 281:291–307. doi:10.1007/s11104-005-4628-7

Blagodatskaya E, Kuzyakov Y (2008) Mechanisms of real and apparent priming effects and their dependence on soil microbial biomass and community structure: critical review. Biol Fertil Soils 45:115–131. doi:10.1007/s00374-008-0334-y

Blagodatskaya E, Kuzyakov Y (2013) Active microorganisms in soil: critical review of estimation criteria and approaches. Soil Biol Biochem 67:192–211. doi:10.1016/j.soilbio.2013.08.024

Blagodatskaya E, Yuyukina T, Blagodatsky S, Kuzyakov Y (2011a) Three-source-partitioning of microbial biomass and of CO_2 efflux from soil to evaluate mechanisms of priming effects. Soil Biol Biochem 43:778–786. doi:10.1016/j.soilbio.2010.12.011

Blagodatskaya E, Yuyukina T, Blagodatsky S, Kuzyakov Y (2011b) Turnover of soil organic matter and of microbial biomass under C3-C4 vegetation change: consideration of ^{13}C fractionation and preferential substrate utilization. Soil Biol Biochem 43:159–166. doi:10.1016/j.soilbio.2010.09.028

Blagodatskaya E, Khomyakov N, Myachina O, Bogomolova I, Blagodatsky S, Kuzyakov Y (2014) Microbial interactions affect sources of priming induced by cellulose. Soil Biol Biochem 74: 39–49. doi:10.1016/j.soilbio.2014.02.017

Blagodatsky S, Blagodatskaya E, Yuyukina T, Kuzyakov Y (2010) Model of apparent and real priming effects: linking microbial activity with soil organic matter decomposition. Soil Biol Biochem 42: 1275–1283. doi:10.1016/j.soilbio.2010.04.005

Bromand S, Whalen J, Janzen H (2001) A pulse-labelling method to generate ^{13}C-enriched plant materials. Plant Soil 235:253–257. doi:10.1023/A:1011922103323

Burns RG, DeForest JL, Marxsen J, Sinsabaugh RL, Stromberger ME, Wallenstein MD, Weintraub MN, Zoppini A (2013) Soil enzymes in a changing environment: current knowledge and future directions. Soil Biol Biochem 58:216–234. doi:10.1016/j.soilbio.2012.11.009

Castellano MJ, Mueller KE, Olk DC, Sawyer JE, Six J (2015) Integrating plant litter quality, soil organic matter stabilization, and the carbon saturation concept. Glob Chang Biol 21:3200–3209. doi:10.1111/gcb.12982

Chen R, Senbayram M, Blagodatsky S, Myachina O, Dittert K, Lin X, Blagodatskaya E, Kuzyakov Y (2014) Soil C and N availability determine the priming effect: microbial N mining and stoichiometric decomposition theories. Glob Chang Biol 20:2356–2367. doi:10.1111/gcb.12475

Chen S, Wang Y, Hu Z, Gao H (2015) CO_2 emissions from a forest soil as influenced by amendments of different crop straws: implications for priming effects. Catena 131:56–63. doi:10.1016/j.catena.2015.03.016

Cotrufo MF, Wallenstein MD, Boot CM, Denef K, Paul E (2013) The microbial efficiency-matrix stabilization (MEMS) framework integrates plant litter decomposition with soil organic matter stabilization: do labile plant inputs form stable soil organic matter? Glob Chang Biol 19:988–995. doi:10.1111/gcb.12113

Cotrufo MF, Soong JL, Horton AJ, Campbell EE, Haddix ML, Wall DH, Parton WJ (2015) Formation of soil organic matter via biochemical and physical pathways of litter mass loss. Nat Geosci 8:776–779. doi:10.1038/ngeo2520

Fontaine S, Mariotti A, Abbadie L (2003) The priming effect of organic matter: a question of microbial competition? Soil Biol Biochem 35: 837–848. doi:10.1016/S0038-0717(03)00123-8

Fontaine S, Barot S, Barré P, Bdioui N, Mary B, Rumpel C (2007) Stability of organic carbon in deep soil layers controlled by fresh carbon supply. Nature 450:277–280. doi:10.1038/nature06275

Garcia-Pausas J, Paterson E (2011) Microbial community abundance and structure are determinants of soil organic matter mineralisation in the presence of labile carbon. Soil Biol Biochem 43:1705–1713. doi:10.1016/j.soilbio.2011.04.016

Guenet B, Neill C, Bardoux G, Abbadie L (2010) Is there a linear relationship between priming effect intensity and the amount of organic matter input? Appl Soil Ecol 46:436–442. doi:10.1016/j.apsoil.2010.09.006

Hayes JM (2004) An introduction to isotopic calculations. Woods Hole, MA 02543, USA: http://www.whoi.edu/cms/files/jhayes/2005/9/IsoCalcs30Sept04_5183.pdf.

Horvath RS (1972) Microbial co-metabolism and the degradation of organic compounds in nature. Bacteriol Rev 36:146–155

Hoyle FC, Murphy DV, Brookes PC (2008) Microbial response to the addition of glucose in low-fertility soils. Biol Fertil Soils 44:571–579. doi:10.1007/s00374-007-0237-3

Jenkinson DS, Fox RH, Rayner JH (1985) Interactions between fertilizer nitrogen and soil nitrogen—the so-called 'priming' effect. J Soil Sci 36:425–444. doi:10.1111/j.1365-2389.1985.tb00348.x

Jiang-shan Z, Jian-fen G, Guang-shui C, Wei Q (2005) Soil microbial biomass and its controls. J Forest Res 16:327–330. doi:10.1007/BF02858201

Johnson JMF, Novak JM, Varvel GE, Stott DE, Osborne SL, Karlen DL, Lamb JA, Baker J, Adler PR (2014) Crop residue mass needed to maintain soil organic carbon levels: can it be determined? BioEnergy Res 7:481–490. doi:10.1007/s12155-013-9402-8

Kramer S, Marhan S, Ruess L, Armbruster W, Butenschoen O, Haslwimmer H, Kuzyakov Y, Pausch J, Scheunemann N, Schoene J, Schmalwasser A (2012) Carbon flow into microbial and fungal biomass as a basis for the belowground food web of agroecosystems. Pedobiologia 55:111–119. doi:10.1016/j.pedobi.2011.12.001

Kuzyakov Y (2010) Priming effects: interactions between living and dead organic matter. Soil Biol Biochem 42:1363–1371. doi:10.1016/j.soilbio.2010.04.003

Kuzyakov Y, Friedel JK, Stahr K (2000) Review of mechanisms and quantification of priming effects. Soil Biol Biochem 32:1485–1498. doi:10.1016/S0038-0717(00)00084-5

Ladd JN, Foster R, Nannipieri P, Oades JM (1996) Soil structure and biological activity. In: Stotzky G, Bollag J-M (eds) Soil biochemistry 9. Marcel Dekker, New York, pp 23–78

Lehmann J, Kleber M (2015) The contentious nature of soil organic matter. Nature 528:60–68. doi:10.1038/nature16069

Leifeld J, von Lützow M (2014) Chemical and microbial activation energies of soil organic matter decomposition. Biol Fertil Soils 50:147–153. doi:10.1007/s00374-013-0822-6

Lian T, Wang G, Yu Z, Li Y, Liu X, Jin J (2016) Carbon input from ^{13}C-labelled soybean residues in particulate organic carbon fractions in a Mollisol. Biol Fertil Soils 52:331–339. doi:10.1007/s00374-015-1080-6

Makarov MI, Malysheva TI, Menyailo OV, Soudzilovskaia NA, Van Logtestijn RSP, Cornelissen JHC (2015) Effect of K_2SO_4 concentration on extractability and isotope signature ($\delta^{13}C$ and $\delta^{15}N$) of soil C and N fractions. Eur J Soil Sci 66:417–426. doi:10.1111/ejss.12243

Meyer SL (1975) Data analysis for scientists and engineers. Wiley, New York

Miltner A, Kindler R, Knicker H, Richnow HH, Kästner M (2009) Fate of microbial biomass-derived amino acids in soil and their contribution to soil organic matter. Org Geochem 40:978–985. doi:10.1016/j.orggeochem.2009.06.008

Miltner A, Bombach P, Schmidt-Brücken B, Kästner M (2012) SOM genesis: microbial biomass as a significant source. Biogeochemistry 111:41–55. doi:10.1007/s10533-011-9658-z

Nannipieri P, Johnson RL, Paul EA (1978) Criteria for measurement of microbial growth and activity in soil. Soil Biol Biochem 10:223–229. doi:10.1016/0038-0717(78)90100-1

Nannipieri P, Kandeler E, Ruggiero P (2002) Enzyme activities and microbiological and biochemical processes in soil. In: Burns RG, Dick RP (eds) Enzymes in the environment. Activity, ecology and applications. Marcel Dekker, New York, pp 1–33

Nannipieri P, Giagnoni L, Landi L, Renella G (2011) Role of phosphatase enzymes in soil. In: Bunemann EK, Obreson A, Frossard E (eds) Phosphorus in action, Soil Biology, vol 26. Springer Verlag, Berlin Heidelberg, pp 215–243

Nannipieri P, Giagnoni L, Renella G, Puglisi E, Ceccanti B, Masciandaro G, Fornasier F, Moscatelli MC, Marinari S (2012) Soil enzymology: classical and molecular approaches. Biol Fertil Soils 48:743–762. doi:10.1007/s00374-012-0723-0

Nguyen TT, Marschner P (2016) Soil respiration, microbial biomass and nutrient availability in soil after repeated addition of low and high C/N plant residues. Biol Fertil Soils 52:165–176. doi:10.1007/s00374-015-1063-7

Nottingham AT, Griffiths H, Chamberlain PM, Stott AW, Tanner EVJ (2009) Soil priming by sugar and leaf-litter substrates: a link to microbial groups. Appl Soil Ecol 42:183–190. doi:10.1016/j.apsoil.2009.03.003

Paterson E, Sim A (2013) Soil-specific response functions of organic matter mineralization to the availability of labile carbon. Glob Chang Biol 19:1562–1571. doi:10.1111/gcb.12140

Poirier V, Angers D, Rochette P, Whalen J (2013) Initial soil organic carbon concentration influences the short-term retention of crop-residue carbon in the fine fraction of a heavy clay soil. Biol Fertil Soils 49:527–535. doi:10.1007/s00374-013-0794-6

Pritsch K, Raidl S, Marksteiner E, Blaschke H, Agerer R, Schloter M, Hartmann A (2004) A rapid and highly sensitive method for measuring enzyme activities in single mycorrhizal tips using 4-methylumbelliferone-labelled fluorogenic substrates in a microplate system. J Microbiol Meth 58:233–241. doi:10.1016/j.mimet.2004.04.001

Rasse DP, Rumpel C, Dignac MF (2005) Is soil carbon mostly root carbon? Mechanisms for a specific stabilisation. Plant Soil 269:341–356. doi:10.1007/s11104-004-0907-y

Sanaullah M, Razavi BS, Blagodatskaya E, Kuzyakov Y (2016) Spatial distribution and catalytic mechanisms of β-glucosidase activity at the root-soil interface. Biol Fertil Soils 52:505–514. doi:10.1007/s00374-016-1094-8

Schnecker J, Wild B, Hofhansl F, Alves RJ, Bárta J, Čapek P, Fuchslueger L, Gentsch N, Gittel A, Guggenberger G, Hofer A (2014) Effects of soil organic matter properties and microbial community composition on enzyme activities in cryoturbated arctic soils. PLoS One 9:e94076. doi:10.1371/journal.pone.0094076

Shahbaz M, Kuzyakov Y, Heitkamp F (2016a) Decrease of soil organic matter stabilization with increasing inputs: mechanisms and controls. Geoderma. doi:10.1016/j.geoderma.2016.05.019

Shahbaz M, Kuzyakov Y, Maqsood S, Wendland M, Heitkamp F (2016b) Decadal nitrogen fertilization decreases mineral-associated and subsoil carbon: a 32 year study. Land Degrad Develop. doi:10.1002/ldr.2667

Stewart CE, Moturi P, Follett RF, Halvorson AD (2015) Lignin biochemistry and soil N determine crop residue decomposition and soil priming. Biogeochemistry 124:335–351. doi:10.1007/s10533-015-0101-8

Tian J, Pausch J, Yu G, Blagodatskaya E, Gao Y, Kuzyakov Y (2015) Aggregate size and their disruption affect ^{14}C-labeled glucose mineralization and priming effect. Appl Soil Ecol 90:1–10. doi:10.1016/j.apsoil.2015.01.014

Vance E, Brookes P, Jenkinson D (1987) An extraction method for measuring soil microbial biomass C. Soil Biol Biochem 19:703–707. doi:10.1016/0038-0717(87)90052-6

Wagner GH (1968) Significance of microbial tissue to soil organic matter. In: Isotopes and radiation in soil organic matter studies. FAO/IAEA, Technical meeting, Vienna, pp 197–205

Wang H, Boutton T, Xu W, Hu G, Jiang P, Bai E (2015) Quality of fresh organic matter affects priming of soil organic matter and substrate utilization patterns of microbes. Sci Rep 5:10102. doi:10.1038/srep10102

Wang J, Dokohely ME, Xiong Z, Kuzyakov Y (2016) Contrasting effects of aged and fresh biochars on glucose-induced priming and microbial activities in paddy soil. J Soils Sediments 16:191–203. doi:10.1007/s11368-015-1189-0

Webster R (2007) Analysis of variance, inference, multiple comparisons and sampling effects in soil research. Eur J Soil Sci 58:74–82. doi:10.1111/j.1365-2389.2006.00801.x

Wu J, Joergensen RG, Pommerening B, Chaussod R, Brookes PC (1990) Measurement of soil microbial biomass C by fumigation-extraction—an automated procedure. Soil Biol Biochem 22:1167–1169. doi:10.1016/0038-0717(90)90046-3

Xiao C, Guenet B, Zhou Y, Su J, Janssens IA (2015) Priming of soil organic matter decomposition scales linearly with microbial biomass response to litter input in steppe vegetation. Oikos 124:649–657. doi:10.1111/oik.01728

Xu X, Ouyang H, Richter A, Wanek W, Cao G, Kuzyakov Y (2011) Spatio-temporal variations determine plant-microbe competition for inorganic nitrogen in an alpine meadow. J Ecol 99:563–571. doi:10.1111/j.1365-2745.2010.01789.x